Title	Water sorption-induced crystallization, structural relaxations and strength analysis of relaxation times in amorphous lactose/whey protein systems
Authors	Fan, Fanghui;Mou, Tian;Nurhadi, Bambang;Roos, Yrjö H.
Publication date	2016-10-27
Original Citation	Fan, F., Mou, T., Nurhadi, B. and Roos, Y. H. (2017) 'Water sorption-induced crystallization, structural relaxations and strength analysis of relaxation times in amorphous lactose/whey protein systems', Journal of Food Engineering, 196, pp. 150-158. doi: 10.1016/j.jfoodeng.2016.10.022
Type of publication	Article (peer-reviewed)
Link to publisher's version	10.1016/j.jfoodeng.2016.10.022
Rights	© 2016 Published by Elsevier Inc. This manuscript version is made available under the CC-BY-NC-ND 4.0 license http://creativecommons.org/licenses/by-nc-nd/4.0/ - http://creativecommons.org/licenses/by-nc-nd/4.0/
Download date	2024-04-17 09:16:37
Item downloaded from	https://hdl.handle.net/10468/3369

Title: Water sorption-induced crystallization, structural relaxations and strength analysis of relaxation times in amorphous lactose/whey protein systems

Corresponding Author: Professor. Yrjo H Roos,

Corresponding Author's Institution: University College Cork

First Author: Fanghui Fan

Order of Authors: Fanghui Fan; Tian Mou; Bambang Nurhadi; Yrjo H Roos

Abstract: Water sorption-induced crystallization, α-relaxations and relaxation times of freeze-dried lactose/whey protein isolate (WPI) systems were studied using dynamic dewpoint isotherms (DDI) method and dielectric analysis (DEA), respectively. The fractional water sorption behavior of lactose/WPI mixtures shown at aw ≤ 0.44 and the critical aw for water sorption-related crystallization (aw(cr)) of lactose were strongly affected by protein content based on DDI data. DEA results showed that the α-relaxation temperatures of amorphous lactose at various relaxation times were affected by the presence of water and WPI. The α-relaxation-derived strength parameter (S) of amorphous lactose decreased with aw up to 0.44 aw but the presence of WPI increased S. The linear relationship for aw(cr) and S for lactose/WPI mixtures was also established with R2 > 0.98. Therefore, DDI offers another structural investigation of water sorption-related crystallization as governed by aw(cr), and S may be used to describe real time effects of structural relaxations in noncrystalline multicomponent solids.

1 Water sorption-induced crystallization, structural relaxations and strength analysis of

2 relaxation times in amorphous lactose/whey protein systems

3

4 Fanghui Fan^{1}, Tian Mou^{2}, Bambang Nurhadi^{1} and Yrjö H. Roos^{1} *

5 *^{1} School of Food and Nutritional Sciences; ^{2} School of Mathematical Sciences,*

6 *University College Cork, Cork, Ireland.*

7

8 **Abstract:** Water sorption-induced crystallization, α-relaxations and relaxation times of

9 freeze-dried lactose/whey protein isolate (WPI) systems were studied using dynamic

10 dewpoint isotherms (DDI) method and dielectric analysis (DEA), respectively. The

11 fractional water sorption behavior of lactose/WPI mixtures shown at $a_w \leq 0.44$ and the

12 critical a_w for water sorption-related crystallization ($a_w^{(cr)}$) of lactose were strongly

13 affected by protein content based on DDI data. DEA results showed that the

14 α-relaxation temperatures of amorphous lactose at various relaxation times were

15 affected by the presence of water and WPI. The α-relaxation-derived strength

16 parameter (S) of amorphous lactose decreased with a_w up to 0.44 a_w but the presence of

17 WPI increased S. The linear relationship for $a_w^{(cr)}$ and S for lactose/WPI mixtures was

18 also established with $R^2 > 0.98$. Therefore, DDI offers another structural investigation

19 of water sorption-related crystallization as governed by $a_w^{(cr)}$, and S may be used to

20 describe real time effects of structural relaxations in noncrystalline multicomponent

21 solids.

22

23 ***Keywords,*** Dynamic Dewpoint Isotherms; Crystallization; α-Relaxation; Relaxation

24 Times; Strength; Water Activity

25

26 * Corresponding author. E-mail address: yrjo.roos@ucc.ie (Y.H. Roos). First author. E-mail
27 address: ffh11235813@gmail.com (F. Fan).

1. Introduction

Water is of key importance to food systems affecting processing, microbial safety, sensory perception, and a storage stability and shelf life (Al-Muhtaseb, McMinn, & Magee, 2002; Lodi & Vodovotz, 2008). Water sorption may be affected by time-dependent phenomena, structural transformations, and phase transitions of food solids. Such transitions may affect rates of deteriorative changes and decrease the storage stability of dehydrated foods, e.g., powdered milk (Silalai & Roos, 2011), potato flakes (Turner et al., 2006), and dry pasta (Aguilera, Chiralt, & Fito, 2003; Gowen, Abu-Ghannam, Frias, & Oliverira, 2008). Water sorption isotherms are important to numerous applications, e.g., development of new products (Wang & Brennan, 1991), determination of product stability and shelf life (Jouppila & Roos, 1994), and process design and control (Peng, Chen, Wu, & Jiang, 2007). The dynamic dewpoint isotherm (DDI) method was developed to generate water sorption isotherms using single samples in a dynamically changing water vapor pressure (Yuan, Carter, & Schmidt, 2011). The DDI method developed along with dynamic vapor sorption provides a continuous measurement of water content (c_w) and water activity (a_w). DDI differs from standard saturated salt solution methods (SSM), which measure c_w for equilibrated materials at known a_w (Schmidt & Lee, 2012). Also, DDI makes it possible to generate complete dynamic isotherms with 50 to 200 data points quickly and accurately without long equilibration times which are typical of SSM methods (Yuan et

49 al, 2011 ; Schmidt & Lee, 2012). Therefore, DDI method offers another real-time

50 investigation of water sorption-related material properties, i.e., crystallization and

51 deliquescence (Yao et al., 2011), in food processing as well as for the control of storage

52 stability and shelf life of resultant products.

53

54 Water sorption characteristics, as well as other interactions of food solids with water,

55 are defined by composition of nonfat components, i.e., carbohydrates and proteins

56 (Roos & Drusch, 2015). Characterization of glass formation of complex food solids

57 systems has been of particular interest in recent years (Ibach & Kind, 2007; Babu &

58 Nangia, 2011). Amorphous food materials exist in a supercooled and non-equilibrium

59 state blow their respective equilibrium melting temperature with no well-defined

60 structure. The nonequilibrium state may exhibit an indefinite number of glass structures

61 with varying levels of molecular packing and order. When temperature increases to

62 above glass transition temperature (T_g), a rapid increase of molecular mobility occurs

63 and the glass-forming material transforms to a viscous liquid, which dramatically

64 affects various physicochemical properties of food solids (Slade, Levine, & Reid, 1991;

65 Bhandari & Howes, 1999). Structural relaxations in amorphous food materials around

66 or above the glass transition occur as a result of molecular mobility changes due to

67 variations in external thermodynamic conditions e.g., pressure and temperature. Glass

68 transition may also result internally in materials because of changes in plasticizer or

69   solvent contents, e.g., water, which can induce dramatic changes in solids properties

70   and directly affect processing, storage, bioavailability, and delivery properties of food

71   materials (Yu, Li, & Sun, 2001; Roos & Drusch, 2015). Relaxation times (τ)

72   correspond to the kinetically impeded and time-dependent molecular rearrangements

73   that are responsible for solids structure and properties, e.g., flow characteristics,

74   viscous flow and collapse, mechanical or dielectric properties, and crystallization

75   (Sperling, 2005). Such properties may be used to control the quality and stability of

76   food materials during processing and storage (Champion, Le Meste, & Simatos, 2000).

77

78   The α-relaxation and relaxation times of glass forming food materials around

79   calorimetric T_g could be studied and determined by dielectric analysis (DEA) (Moates,

80   Noel, Parker, & Ring, 2001; Clerjon, Daudin, & Damez, 2003). The α-relaxation

81   temperature (T_α) may also be taken from the dielectric loss (ε'') peak temperature at

82   various frequencies to obtain corresponding relaxation times (Silalai & Roos, 2011).

83   The Williams-Landel-Ferry (WLF) model is often used to model relaxation times of the

84   non-Arrhenius temperature dependence of relaxation processes occurring above T_g,

85   and the τ is shown against T-T_g (Slade, Levine, & Reid, 1991). The WLF-relationship

86   applies over the temperature range covering the rubbery or supercooled liquid state and

87   it was also used to describe time and temperature dependent behavior of food solids

88   systems. The "strength" concept and strength parameter (S) developed by Roos and

89   others (2015) combined the characterization of material state and relaxation times to

90   describe the critical temperature difference at which a sharp change in properties of the

91   material occurs. On the other hand, the S parameter based on WLF modeling was used

92   to describe amorphous food solids and their properties for typical processing and

93   storage conditions where a component or miscible components within food structure

94   may experience the glass transition (Fan & Roos, 2016a). Besides the strength of food

95   solids, the Deborah number was applied to provide a useful translation of measured

96   relaxation times to real timescales. Therefore, the strength concept gives a quantitative

97   measure to estimate compositional effects on relaxation times to describe properties of

98   food solids above measured T_g.

99

100 Lactose (β-D-galactopyranosyl (1–4)-D-glucopyranose) is one of the most common

101 and important ingredients in many formulated foods and pharmaceutical materials, and

102 it exhibits strong water-dependent properties, i.e., glass transition and crystallization

103 from its amorphous states during storage (Nickerson, 1979; Gänzle, Haase, & Jelen,

104 2008). Understanding glass transition-related structural relaxations and their coupling

105 with water sorption properties is essential for modeling the physical state of

106 dairy-based food systems at various conditions and the design of complex formulations.

107 The importance of glass transition to amorphous solids characteristics has been well

108 recognized but few studies have contributed to understanding effects of glass former or

109   polymer, i.e., protein, on the water sorption characteristics and structural relaxations in

110   food formulations. Therefore, the major objective of the present study was to

111   investigate the influence of food polymeric components (whey protein isolates, WPI)

112   on the water sorption properties of freeze-dried amorphous lactose/WPI mixtures using

113   the DDI measurement data at 25 °C. The strength analysis was carried out to determine

114   the S parameter for lactose/WPI systems by analyzing their relaxation times measured

115   by DEA after storage at $a_w \leq 0.44$ a_w and 25 °C. These data are useful for the

116   understanding of the effects of proteins on water sorption properties of amorphous

117   lactose and collective structural relaxation behavior when present with amorphous

118   lactose around the glass transition in well-mixed food and pharmaceutical materials.

119

120   **2. Materials and Methods**

121   **2.1. Sample preparation**

122

123   α-Lactose monohydrate (>99 % lactose) (Sigma-Aldrich, St. Louis, Mo., U.S.) and

124   whey protein isolate (WPI; Isolac®, Carbery Food Ingredients, Co., Ballineen, Ireland;

125   minor components including carbohydrates or lipids < 3%) were used. Aqueous lactose

126   and WPI with 20 % (mass) solids at room temperature were used to obtain ratios of 7:3,

127   1:1 and 3:7 of lactose/WPI by mass. Mixed solutions (5 mL in total) were prepared in

128   pre-weighted glass vials (10 mL; Schott Müllheim, Germany). All solutions in the vials

129 (semi-closed with septum) were frozen at -20 °C for 20 h and then subsequently

130 tempered at -80 °C for 3 h prior to freeze-drying using a laboratory freeze-dryer

131 (Lyovac GT2 Freeze-Dryer, Amsco Finn-Aqua GmbH, Steris[®], Hürth, Germany).

132 After freeze-drying at pressure < 0.1 mbar, triplicate samples of each material were

133 stored in evacuated desiccators over P_2O_5 at 25 °C (Sigma-Aldrich, St. Louis, Mo.,

134 U.S.) prior to subsequent analysis.

135

136 **2.2. Water sorption experiment**

137

138 The water sorption of freeze-dried samples was studied using an AquaSorp isotherm

139 generator (AIG; Decagon Devices, Inc. Pulman WA, USA). The airflow

140 continuously passes over the sample in AIG until certain interval time or when there

141 was a mass or a_w change of sample, then the flow stopped and the snapshot of the

142 sorption process was taken by directly measuring mass and a_w based on a high precision

143 magnetic force balance and chilled-mirror dewpoint sensor (Decagon Devices, Inc.

144 Pulman WA, USA). Based on above principle the dynamic water sorption of DDI can

145 be comparable to real-time sorption process for a material with fast vapor diffusion or

146 by reducing the sample size. In the present study, approximately 600 mg of each sample

147 (dried powder), which could cover the bottom of stainless steel sample cup, was used in

148 measurements. Measurement parameters were 0.05 to 0.90 a_w at a temperature of 25 °C,

149 airflow of 300 ml/min (Schmidt & Lee, 2012). At certain interval time, the airflow

150 stopped automatically then the weight change and the a_w of the sample were recorded.

151 After initial c_w was determined, the mass was converted to the c_w of the sample at the

152 corresponding a_w and a plot of the dynamic sorption isotherm using the SorpTrac

153 software, version 1.03.3 (Decagon Devices, Pullman, WA, USA) was generated. Since

154 each DDI run is unique, the sorption section of the working isotherm was obtained in

155 duplicate, each on a different sample.

156

157 Fig 1.

158

159 The critical a_w value for water sorption-induced crystallization ($a_w^{(cr)}$) of lactose and

160 lactose/WPI mixtures were analyzed and determined by calculating the changes of c_w in

161 DDI of each sample using derivative analysis (Yuan et al., 2011). The procedures used

162 to obtain the first and the second derivative was as follows. Attempts to leave out noise

163 and find the peak location, the a_w and c_w data derived from DDI were smoothed using

164 LOESS (local polynomial regression fitting) smoothing (second-degree polynomial)

165 with a span of 11 points using the R programme, version 3.2.3 (The R Foundation[©],

166 Murray Hill, NJ, USA). The smoothed data set was fit using a smoothing cubic spline

167 after which the first derivative of the fit was taken. The peak a_w of the 1st derivative

168 function ($a_{wp}^{(cr)}$) based on smoothed DDI data was taken as acceleration point for

169   lactose crystallization. The smoothing and fitting procedures were repeated for the 1st

170   derivative after which the 2nd derivative was obtained from the 1st derivative. Water

171   sorption data showed that a substantial peak on the 2nd derivative developed with onset

172   around the calorimetric T_g corresponding a_w, $a_{wo}^{(cr)}$ (Fig. 1A). The water plasticization

173   to above the glass transition induced translational mobility of lactose. Such mobility

174   with further water plasticization could increase free volume to provide water sorption

175   sites and hydrogen bonding structuring of the lactose-water system to accommodate

176   water with less direct lactose-lactose interactions. The programmed codes for achieving

177   first and second derivative analysis in R programme were shown on Supplementary

178   Information.

179

180   **2.3. Dielectric analysis (DEA)**

181

182   DEA was used to measure dielectric properties from the dielectric constant or

183   permittivity (ε'), dielectric loss (ε''), and their ratio tan $\delta = (\varepsilon''/\varepsilon')$ as a function of

184   temperature. The ε' describes an alignment of dipoles and the ε'' describes an energy

185   that is required to align dipoles (Talja & Roos, 2001). In the present study, the

186   freeze-dried lactose and lactose/WPI at 7:3, 1:1 and 3:7 mass ratios were humidified for

187   120 h over saturated solutions of CH_3COOK, $MgCl_2$, and K_2CO_3 (Sigma Chemical Co.,

188   St. Louis, Mo., USA) to obtain respective water activities of 0.23, 0.33 and 0.44 a_w at

189   equilibrium in vacuum desiccators in incubators at storage temperature of 25 °C.

190   Dielectric properties of both dry and humidified samples were analyzed using dielectric

191   analyzer (DS6000, Triton Technology Ltd., UK), with titanium sample holders as the

192   electrodes. The LCR meter (inductance, capacitance, and resistance; LCR-819) and

193   DEA instrument were calibrated and zeroed with the open-short circuit of the

194   electrodes before starting experiments. Samples were ground and approximately 600

195   mg samples were placed between parallel plate titanium capacitors (diameter = 33 mm)

196   with the thickness less than 2 mm. Triplicate samples of each material were analyzed

197   using dynamic measurements and recorded using Triton Laboratory software (version

198   1.0.330). Samples were analyzed in triplicate using dynamic measurements and

199   scanned from ~ 60 °C below to over the T_g region with cooling rate of 5 °C/min and

200   heating rate of 2 °C/min at frequencies of 0.5, 1.0, 5.0, 10.0 and 20.0 kHz. The

201   measuring head was connected to a liquid nitrogen tank (1L; Cryogun, Brymill

202   cryogenic systems, Labquip (Ireland) Ltd., Dublin, Ireland). As noted above, T_α

203   determined from the temperature of ε'' at the peak were used to determine the relaxation

204   times.

205

206   **2.4. Strength analysis**

207

208   The relaxation times and T_α corresponding to ε'' peak above T_g were modeled using the

209   WLF equation (Eq. 1). The relaxation times were defined by frequency set in DEA

210   measurements ($\tau = 1/2\pi f$). The WLF model constants C_1 and C_2 were derived from a

211   plot of $1/log(\tau/\tau_g)$ against $1/(T-T_g)$ using experimental τ with the assumption of $\tau_g = 100$

212   s at the calorimetric onset temperature of the T_g (Angell 2002). A decrease in the

213   number of logarithmic decades for flow, e.g., that being critical for stickiness, could be

214   used as the critical parameter, d_s, of Eq. (2) and the corresponding T-T_g was defined as

215   the strength of the solids, S. As the S values are given as temperature corresponding to a

216   critical τ for a key amorphous component within a material, it also provides a measure

217   of resistance to structural changes, i.e., the higher value of S refers to a stiffer system at

218   a corresponding T-T_g.

219

220    $$log\left(\frac{}{g}\right) = \frac{C_1(T \quad T_g)}{C_2 + (T \quad T_g)} \qquad (1)$$

221    $$S = \frac{d_s C_2}{C_1 \quad d_s} \qquad (2)$$

222

223   Where, T, T_g, τ, τ_g, C_1 and C_2 and d_s shown in Eq (1) and (2) refer to the experimental

224   temperature, onset glass transition temperature, experimental structural relaxation time

225   and structural relaxation time at the glass transition ($\tau_g = 100$ s), material-specific WLF

226   constants and the decrease in the number of logarithmic decades for τ ($d_s = 4$ was used

227 for various biological materials as reported by Roos et al. (2015) and Fan and Roos

228 (2016b), respectively.

229

230 **2.6. Statistical analysis**

231

232 The second derivative analysis of DDIs sorption data was carried out in *R* Programme

233 and the strength analysis of dielectric α-relaxation associated relaxation times were

234 calculated and fitted by using Microsoft Office Excel 2011 (Microsoft, Inc., USA). All

235 measurements were repeated three times, as well as the average values with the

236 standard deviation of triplicate measurements were calculated.

237

238 **3. Results and Discussion**

239 **3.1. Dynamic Water Sorption**

240

241 Table 1 and Fig. 2

242

243 The DDI for pure lactose ($a_w \leq 0.50$), WPI and lactose/WPI mixtures with the mass

244 ratios of 7:3 ($a_w \leq 0.70$), 1:1 ($a_w \leq 0.80$) and 3:7 followed the typical sigmoid shape of

245 water sorption isotherms (type II) in Fig. 1B, respectively. The fractional water

246 sorption of components, exhibited by amorphous sugar/protein mixtures, has been

247   reported by previous studies (Roos & Potes, 2015). Similarly, the fractional water

248   sorption properties were proved in DDIs as the sorbed water in amorphous lactose/WPI

249   mixtures could be calculated as the sum of fractional quantities at $a_w \leq 0.44$ (Fig. 1B).

250   However, if water sorption rates of components vary DDI data may reflect such

251   differences. Fig. 2 gives the DDI water sorption and literature SSM data for

252   freeze-dried lactose and lactose/WPI mixtures at 7:3, 1:1 and 3:7 mass ratios at 25 °C

253   (Fan & Roos, 2015). The water contents in DDIs of lactose were lower than those of

254   corresponding SSM isotherms (Fig. 2A). Such differences in the DDI sorption data

255   reflected the non-equilibrium state of amorphous solids and the relatively short

256   equilibration time in comparison to SSM giving a systematic error for the water content

257   as full dehydration may not take place at low a_w. The SSM-isotherms comparable c_w

258   data are shown on the DDIs of lactose/WPI mixtures at various protein contents (Fig.

259   2B-D). The DDI sorption data of pure amorphous WPI, however, showed

260   shape-comparable sorption isotherms to corresponding SSM isotherms (Fig. 2E). Such

261   similarity in water sorption by the two methods indicated that the amorphous WPI

262   showed a slow equilibration reducing time to water vapor diffusion and water

263   penetration during DDI sorption. The DDI sorption data for amorphous lactose leveled

264   off at high water activities (≥ 0.50 a_w) as a result of lactose crystallization (Fig. 2A). In

265   lactose/WPI systems lactose molecules form a continuous phase around WPI

266   molecules, but WPI components may hinder diffusion of the noncrystalline lactose. In

267   comparison to pure lactose, therefore, the presence of WPI in lactose/WPI mixtures

268   delayed crystallization and extended the sigmoid sorption behaviors to a higher a_w

269   range (Fig. 2B-C). This phenomenon agreed with previous studies, which indicated that

270   the crystallization of lactose could be delayed by the presence of polymeric

271   components (Silalai & Roos, 2011). As noted above, the presence of other components,

272   e.g., protein, with amorphous sugars, affected water sorption as well as the

273   crystallization as a result of water plasticization.

274

275   Fig. 3

276

277   The $a_w^{(cr)}$ values of amorphous lactose and lactose/WPI mixtures at each ratio are

278   shown in Table 1, respectively. Fig. 2F showed a linear relationship with high

279   correlation coefficient ($R^2 > 0.98$) for $a_w^{(cr)}$ values against lactose content of amorphous

280   lactose/WPI systems at 25 °C, which indicated that the $a_w^{(cr)}$ was that of the lactose

281   component rather than for the entire system although protein affected structural

282   relaxation times (Roos & Potes, 2015). In the present study, the $a_{wo}^{(cr)}$ was considered

283   as a critical a_w point for glass-forming lactose plasticized by water to flow and

284   accommodate increasing free volume and water uptake during DDI sorption process.

285   The $a_{wp}^{(cr)}$ was a turning point where the rate of water uptake became less than the rate

286   of lactose crystallization. Corresponding to previous X-ray study (Jouppila et al., 1997),

287   therefore, we assumed that the $a_{wo}^{(cr)}$ and $a_{wp}^{(cr)}$ were the onset and half-crystallinity

288   point of lactose crystallization, respectively. In the present study, the $a_{wo}^{(cr)}$ of pure

289   amorphous lactose occurred at 0.381 a_w at 25 °C (Table 1). This result agreed with

290   previous calorimetric studies that the glass transition of freeze-dried lactose after

291   humidification at 0.44 a_w at room temperature was around 15 °C as well as the critical

292   a_w of 0.37 of amorphous lactose (Fan & Roos, 2016a). Both onset and peak $a_w^{(cr)}$ values

293   of lactose/WPI mixtures increased concomitantly with increasing protein content

294   (Table 1). Fig. 3 gives a schematic diagram for the dynamic water sorption process of

295   amorphous lactose and lactose/WPI mixtures. From I to II (Fig. 3A), the water sorbed

296   by amorphous lactose could plasticize the structure of glass formers resulting in

297   breaking the hydrogen bonds between lactose molecules and the relaxation times of

298   amorphous lactose decreased (Slade et al., 1991). As a_w increased to above $a_{wo}^{(cr)}$, the

299   mobilization of glass formers was strongly enhanced by water plasticization (Fig. 3A

300   II-III). When the a_w exceeded $a_{wp}^{(cr)}$, the lactose crystallinity rapidly increased until

301   most of lactose crystallized during the DDI sorption process (Fig. 3A III-IV). However,

302   the presence of WPI hindered water plasticization effects as the $a_{wo}^{(cr)}$ increased in

303   lactose/WPI mixtures (Fig. 3B II-III). Moreover, the $a_{wp}^{(cr)}$ of lactose/WPI mixtures

304   increased concomitantly with the WPI content and delayed the lactose crystallization in

305   mixtures (Fig. 3B III-IV). Therefore, the $a_w^{(cr)}$ values of the DDI data indicate the glass

306   transition resulting in mobilization and crystallization of amorphous lactose in food and

307   pharmaceutical materials.

308

309 **3.2. Dielectric properties and T_α**

310

311 Table 2 and Fig. 4

312

313 Fig. 4 shows the dielectric loss (ε'' peaks at a frequency of 1.0 kHz) for lactose and

314 lactose/WPI mixtures with mass ratios of 7:3, 1:1 and 3:7 after storage below 0.44 a_w at

315 25 °C. Dielectric properties of the materials were affected by molecular interactions

316 and water plasticization. The magnitude of the ε'' peak correlated directly to a_w of

317 amorphous lactose at low water activities ($0.23 \leq a_w \leq 0.44$) as water content increased

318 and plasticization enhanced the mobility of lactose molecules. This agreed with Silalai

319 and Roos (2011) who reported that ε'' peaks found for skim milk powder increased in

320 magnitude with increasing a_w (Fig. 4A). The ε'' describes an energy loss that is used by

321 polar groups in materials under the alternating electric field. The lower levels of WPI

322 containing lactose/WPI mixtures ($\leq$ 30 %) showed higher magnitudes of ε'' peaks than

323 pure lactose after humidification at the same a_w and 25 °C (Fig. 4B-D). Therefore, the ε''

324 data followed the amorphous lactose content of the mixtures as WPI and lactose exist in

325 separate phases. Table 2 gives the T_α value of each material in dielectric analysis at 1.0

326 kHz, which occurred above the corresponding calorimetric onset T_g measured by

327 differential scanning calorimeter (DSC) in agreement with Silalai and Roos (2011).

328 The presence of water, in the present study, decreased the T_α values of amorphous

329 lactose and lactose/WPI mixtures as the peak temperature of ε'' concomitantly

330   decreased with increasing a_w (Table 2). The T_α values of amorphous lactose could be

331   significantly increased by WPI in lactose/WPI mixtures (Table 2). Lactose can be

332   assumed to exist separated from protein. The frequency-dependent T_α indicated an

333   apparent relaxation time of lactose in WPI mixtures. Water plasticization enhanced the

334   molecular mobility of lactose molecules which consequently decreased the peak

335   temperature of ε''. However, the WPI contained in mixtures hindered the molecular

336   mobility of lactose and increased the apparent relaxation times and T_α. In our previous

337   studies, similarly, the presence of other components, i.e., water and protein, affected

338   the structural relaxations, relaxation times and T_α of glass-forming sugars in

339   freeze-dried sugars/protein systems based on dynamic-mechanical analysis (DMA)

340   (Fan & Roos, 2016a,b).

341

342   **3.3. Relaxation times and *S* parameter**

343

344   Fig. 5

345

346   Both DEA and DMA measurements allowed determination of structural relaxation

347   times from the α-relaxation data at various frequencies. The structural relaxation times

348   can be related to stickiness characteristics of food powders as well as other mechanical

349   properties of food solids, such as the collapse of structure or viscosity and diffusion

350   (Clerjon et al., 2003). Fig. 5 shows structural relaxation times from our experiments

351   and literature (Fan & Roos, 2016a). The WLF-relationship of Williams et al. (1955)

352   was developed on the basis that most inorganic and organic glass formers showed

353   similar decreases in τ and viscosity over the temperature range of T_g to T_g+100K. The

354   use of WLF-relationships often assumes that the structural relaxation time obtained

355   using dielectric measurements reach 100 s at the calorimetric onset T_g (Angell, 2002;

356   Roos et al., 2015). In the present study, the WLF-relationship with "universal"

357   constants (C_1 = -17.44 and C_2 = 51.6) did not fit the experimental data but

358   material-specific constants gave a good fitting performance for lactose and lactose/WPI

359   mixtures at a_w below 0.44 and 25 °C (Fig. 5). Table 2 gives material-specific WLF

360   constants for amorphous lactose and lactose/WPI mixtures obtained from structural

361   relaxation times of the DEA and published DMA measurements. The material-specific

362   C_1 for amorphous lactose increased concomitantly with a_w increasing, whereas both C_1

363   and C_2 decreased by the presence of WPI content at a_w below 0.44 (Table 2). It is

364   important to note that fitting of the WLF model to experimental relaxation times may

365   result in positive or negative values or negative values for the constants C_1 and C_2

366   (Roos & Drusch, 2015). In the present study, the C_1 and C_2 with negative values

367   determined the downward concavity for WLF relationship, which showed the profiles

368   for the decreases of relaxation times of amorphous lactose at temperatures above

369   calorimetric T_g. Therefore, the material-specific WLF constants could be used to

370   describe material properties and structural relaxation processes of amorphous lactose at

371   various water activities. The presence of other components, e.g., water and protein,

372   affected the structural overall relaxation processes as well as apparent relaxation times

373   of lactose/WPI mixtures.

374

375   The decrease of relaxation times to 10^{-2} corresponded to a decrease in viscosity from

376   10^{12} Pa s to 10^{5} Pa s reaching critical viscosities for collapse and stickiness of

377   amorphous food solids (Bellows & King, 1973; Downton, Flores-Luna, & King, 1982).

378   Roos et al. (2015) recommended a WLF model-based strength analysis for amorphous

379   sugars/protein systems. The S parameter for glass-forming components calculated by

380   using material-specific WLF constants defined an allowable increase in temperature

381   above the onset of the calorimetric T_g until $\tau = 0.01$ s. As the lactose and protein

382   diffusion was uncoupled the S parameter followed relaxation times of amorphous

383   lactose. Table 2 gives the S values of amorphous lactose and lactose/WPI mixture at

384   low a_w based on the strength analysis using experimental structural relaxation times

385   derived from DEA and published DMA data. In the present study, the S values of

386   freeze-dried lactose with different water activities agreed with our earlier data (Fan &

387   Roos, 2016a). The presence of water decreased the structural strength of amorphous

388   lactose at a_w below 0.44, whereas the S values of lactose/WPI mixtures were

389   significantly higher than was found for pure lactose (Table 2). As the S parameter

390   provides a measure of structural transformation, a low S value referred to a more rapid

391   structural change. Such rapid changes occurred in the presence of water as the

392   structural relaxations of amorphous lactose were enhanced by water plasticization.

393   However, the relatively higher S exhibited by lactose/WPI mixtures indicated that the

394   mixes were strengthened against structural deformation as protein offered a structural

395   supporting effect. Therefore, the S parameters based on dielectric/mechanical

396   relaxations can be used to describe compositional effects of amorphous food solids

397   systems. Such data can be used to control shrinkage in dehydration and possibly rates

398   of physicochemical changes in food storage.

399

400   **3.4. Sorption-induced crystallization, relaxation times and S parameter**

401

402   Fig. 6

403

404   The relationships between a_w and $T\text{-}T_g$ of amorphous lactose and lactose/WPI mixtures

405   against their corresponding relaxation times are shown in Fig. 6A. The water-induced

406   structural relaxations of food solids systems, observed in isothermal water sorption, are

407   likely to correlate with crystallization above glass transition. The relaxation times of

408   lactose dramatically decreased with increasing $T\text{-}T_g$ as the T_g was depressed by water

409   (Fig. 6A). The crystallization of lactose was initialized above $a_{wo}^{(cr)}$ and rapidly

410   occurred along decreasing structural relaxation times during water sorption process.

411   The water sorption-induced lactose crystallization could stop at 0.7 a_w based on the

412   DDI sorption data, where the τ decreased approximately 4 logarithmic decades (Fig.

413   6A). As we expected, the $a_{wo}^{(cr)}$ for water-induced crystallization was delayed to occur

414   at higher a_w in the presence of WPI (Fig. 6A). The decrease of structural relaxation

415   times, $a_{wp}^{(cr)}$ and crystallization of amorphous lactose can be controlled by WPI during

416   exposures to high humidities (Fig. 6A). Fig. 6B shows a plot of onset and peak $a_w^{(cr)}$

417   against S for anhydrous lactose and lactose/WPI mixtures. There was a linear

418   relationship between $a_w^{(cr)}$ and S with high correlation ($R^2 > 0.97$). The pure lactose had

419   a lower $a_w^{(cr)}$ and S value than WPI containing systems (Fig. 6B). This result indicated

420   that the structural strength could be related to water-induced crystallization of

421   amorphous sugars during isothermal water sorption. Therefore, we believe that the DDI

422   provided parameters describe the structural changes and crystallization behavior of

423   amorphous sugars during water plasticization. The S parameter could be used to

424   estimate time-dependent water sorption-induced solid properties of amorphous food

425   mixtures during storage at various water activities, i.e., structural transformations and

426   deformation. Moreover, proteins as commonly used components could be used in food

427   and pharmaceutical systems to control water sorption properties as well as structural

428   relaxation rates and crystallization.

429

4. Conclusion

We have shown that the freeze-dried lactose and lactose/WPI mixtures have fractional water sorption properties. Water sorption-induced relaxations and crystallization were delayed in the presence of WPI in amorphous lactose/WPI mixtures. The T_α values of amorphous lactose in lactose/WPI mixtures at $a_w \leq 0.44$ were affected by the mixture composition, i.e., water, and WPI. The WLF analysis based S parameter with relaxation times data from DEA and DMA was dependent on mixture composition. It was used to interpret water sorption-induced crystallization of amorphous lactose in mixtures with WPI. The combination of dielectric and mechanical properties offers a new approach in understanding glass transition-related structural relaxations occurring in food processing and storage. Such information also advances innovations in food formulation through mapping of structural relaxation times of food components and their mixes.

451

452

453

454

455

456

457

458

459

460

461

462

463

464

465

466

467

468   ***References***

469

470   Aguilera, J. M., Chiralt, A., & Fito, P. (2003). Food dehydration and product structure.

471   *Trends in Food Science & Technology, 14*(10), 432-437.

472   Al-Muhtaseb, A. H., McMinn, W. A. M., & Magee, T. R. A. (2002). Moisture sorption

473   isotherm characteristics of food products: a review. *Food and Bioproducts*

474   *Processing, 80*(2), 118-128.

475   Angell, C. A. (2002). Liquid fragility and the glass transition in water and aqueous

476   solutions. *Chemical Reviews, 102*(8), 2627-50.

477   Babu, N. J., & Nangia, A. (2011). Solubility advantage of amorphous drugs and

478   pharmaceutical cocrystals. *Crystal Growth & Design, 11*(7), 2662-79.

479   Bellows, R. J., & King, C. J. (1973). Product collapse during freeze drying of liquid

480   foods. *AIChE Symposium Series, 132*(69), 33-41.

481   Bhandari, B. R., & Howes, T. (1999). Implication of glass transition for the drying and

482   stability of dried foods. *Journal of Food Engineering, 40*(1), 71-79.

483   Champion, D., Le Meste, M., & Simatos, D. (2000). Towards an improved

484   understanding of glass transition and relaxations in foods: molecular mobility in the

485   glass transition range. *Trends in Food Science & Technology, 11*(2), 41-55.

486   Clerjon, S., Daudin, J. D., & Damez, J. L. (2003). Water activity and dielectric

487   properties of gels in the frequency range 200 MHz–6 GHz. *Food Chemistry, 82*(1),

488   87-97.

489   Downton, G. E., Flores-Luna, J. L., & King, C. J. (1982). Mechanism of stickiness in

490   hygroscopic, amorphous powders. *Industrial & Engineering Chemistry*

491   *Fundamentals, 21*(4), 447-451.

492   Fan, F., & Roos, Y. H. (2015). X-ray diffraction analysis of lactose crystallization in

493   freeze-dried lactose–whey protein systems. *Food Research International, 67*, 1-11.

494   Fan, F., & Roos, Y. H. (2016a). Structural relaxations of amorphous lactose and

495   lactose-whey protein mixtures. *Journal of Food Engineering, 173*, 106-115.

496   Fan, F., & Roos, Y. H. (2016b). Crystallization and structural relaxation times in

497   structural strength analysis of amorphous sugar/whey protein systems. *Food*

498   *Hydrocolloids, 60*, 85-97.

499   Gänzle, M. G., Haase, G., & Jelen, P. (2008). Lactose: crystallization, hydrolysis and

500   value-added derivatives. *International Dairy Journal, 18*(7), 685-694.

501   Gowen, A. A., Abu-Ghannam, N., Frias, J., & Oliveira, J. (2008). Modelling

502   dehydration and rehydration of cooked soybeans subjected to combined

503   microwave-hot air-drying. *Innovative Food Science & Emerging Technologies, 9*(1),

504   129-137.

505   Ibach, A., & Kind, M. (2007). Crystallization kinetics of amorphous lactose,

506   whey-permeate and whey powders. *Carbohydrate Research, 342*(10), 1357-1365.

507   Jouppila, K., & Roos, Y. H. (1994). Glass transitions and crystallization in milk

508   powders. *Journal of dairy science, 77*(10), 2907-2915.

509   Jouppila, K., Kansikas, J., & Roos, Y. H. (1997). Glass transition, water plasticization,

510   and lactose crystallization in skim milk powder. *Journal of Dairy Science, 80*(12),

511   3152-60.

512   Lodi, A., & Vodovotz, Y. (2008). Physical properties and water state changes during

513   storage in soy bread with and without almond. *Food Chemistry, 110*(3), 554-561.

514   Moates, G. K., Noel, T. R., Parker, R., & Ring, S. G. (2001). Dynamic mechanical and

515   dielectric characterisation of amylose–glycerol films. *Carbohydrate Polymers*, *44*(3),

516   247-253.

517   Nickerson, T. A. (1979). Lactose chemistry. *Journal of Agricultural and Food*

518   *Chemistry, 27*(4), 672-677.

519   Peng, G., Chen, X., Wu, W., & Jiang, X. (2007). Modelling of water sorption isotherm

520   for corn starch. *Journal of Food Engineering, 80*(2), 562-567.

521   Roos, Y .H., Fryer, P. J., Knorr, D., Schuchmann, H. P., Schroën, K., Schutyser, M. A.

522   I., Trystram, G., Windhab, E. J. (2015). Food engineering at multiple scales: case

523   studies, challenges and the future - a European perspective. *Food Engineering*

524   *Review*. *8*(91), 91-115.

525   Roos, Y. H., & Potes, N. (2015). Quantification of Protein Hydration, Glass

526   Transitions, and Structural Relaxations of Aqueous Protein and

527   Carbohydrate–Protein Systems. *The Journal of Physical Chemistry B, 119*(23),

528   7077-86.

529   Roos, Y.H., & Drusch, S. (2015). *Phase Transitions in Foods*, Second ed. Academic

530   Press, Inc., San Diego.

531   Schmidt, S. J., & Lee, J. W. (2012). Comparison between water vapor sorption

532   isotherms obtained using the new dynamic dewpoint isotherm method and those

533   obtained using the standard saturated salt slurry method. *International Journal of*

534   *Food Properties, 15*(2), 236-248.

535   Silalai, N., & Roos, Y. H. (2011). Coupling of dielectric and mechanical relaxations

536   with glass transition and stickiness of milk solids. *Journal of Food Engineering,*

537   *104*(3), 445-454.

538   Slade, L., Levine, H., & Reid, D. S. (1991). Beyond water activity: recent advances

539   based on an alternative approach to the assessment of food quality and safety. *Critical*

540   *Reviews in Food Science & Nutrition, 30*(2-3), 115-360.

541   Sperling, L. H. (2005). *Introduction to physical polymer science*. John Wiley & Sons.

542   Talja, R. A., & Roos, Y. H. (2001). Phase and state transition effects on dielectric,

543   mechanical, and thermal properties of polyols. *Thermochimica Acta, 380*(2), 109-121.

544   Turner, N. J., Whyte, R., Hudson, J. A., & Kaltovei, S. L. (2006). Presence and growth

545   of Bacillus cereus in dehydrated potato flakes and hot-held, ready-to-eat potato

546   products purchased in New Zealand. *Journal of Food Protection, 69*(5), 1173-77.

547   Wang, N., & Brennan, J. G. (1995). A mathematical model of simultaneous heat and

548   moisture transfer during drying of potato. *Journal of Food Engineering, 24*(1), 47-60.

549   Williams, M. L., Landel, R. F., & Ferry, J. D. (1955). The temperature dependence of

550   relaxation mechanisms in amorphous polymers and other glass-forming liquids.

551   *Journal of the American Chemical Society, 77*(14), 3701-3707.

552   Yao, W., Yu, X., Lee, J. W., Yuan, X., & Schmidt, S. J. (2011). Measuring the

553   deliquescence point of crystalline sucrose as a function of temperature using a new

554   automatic isotherm generator. *International Journal of Food Properties, 14*(4),

555   882-893.

556   Yu, K. Q., Li, Z. S., & Sun, J. (2001). Polymer structures and glass transition: A

557   molecular dynamics simulation study. *Macromolecular theory and simulations,*

558   *10*(6), 624-633.

559   Yuan, X., Carter, B. P., & Schmidt, S. J. (2011). Determining the critical relative

560   humidity at which the glassy to rubbery transition occurs in polydextrose using an

561   automatic water vapor sorption instrument. *Journal of Food Science, 76*(1), 78-89.
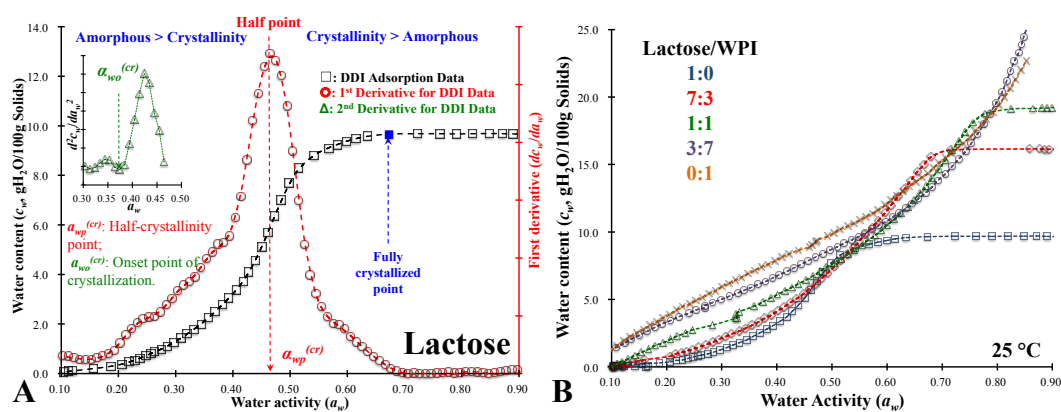
562

Figure 1. The $a_w^{(cr)}$ for freeze-dried lactose respectively taking the peak a_w of first derivative ($a_{wp}^{(cr)}$) and onset a_w of the second derivative ($a_{wo}^{(cr)}$) on DDI sorption data at 25 °C (A). B shows the DDI curves for lactose and lactose/WPI mixtures with 7:3, 1:1 and 3:7 mass ratios by running at 25 °C, respectively.
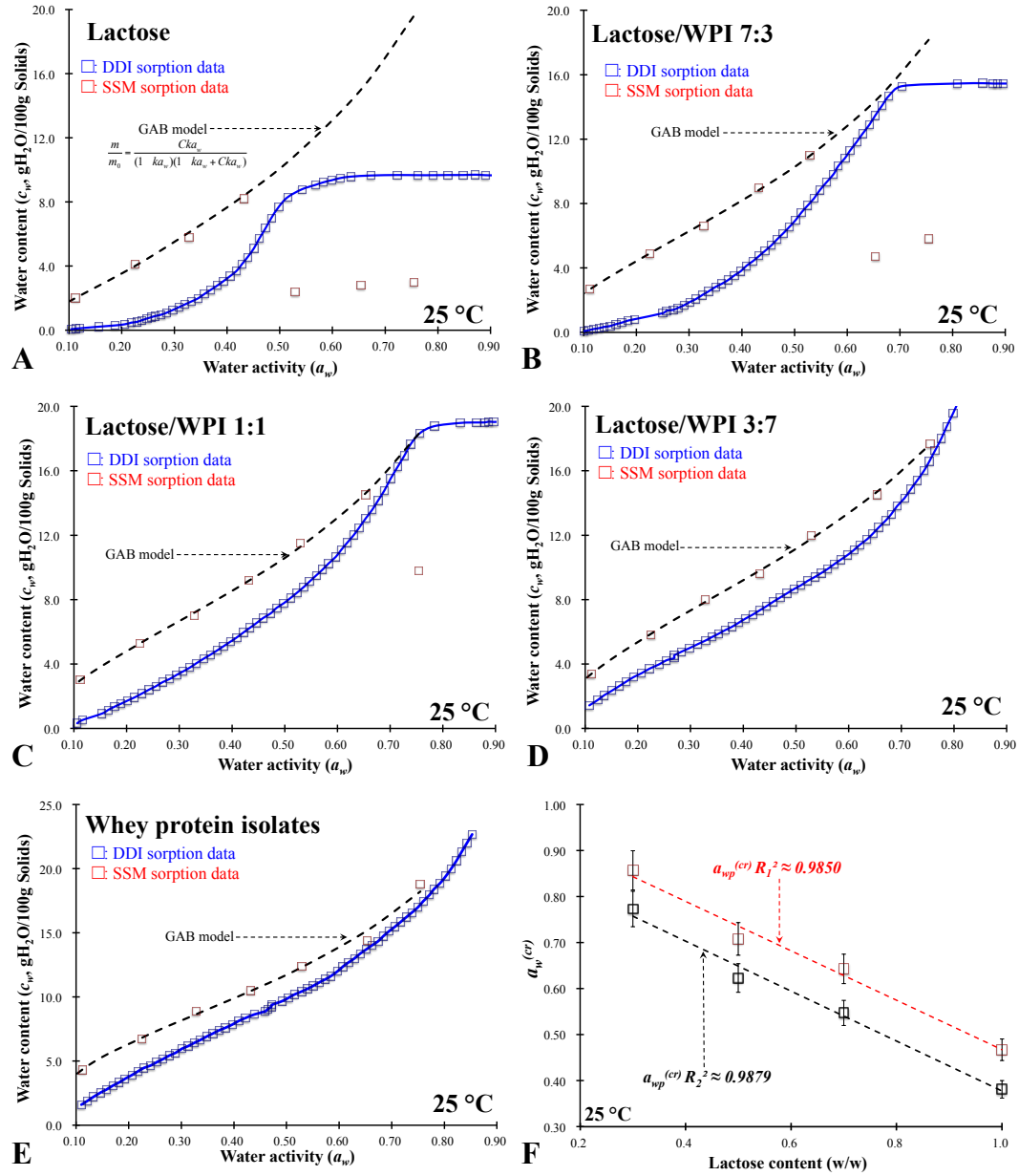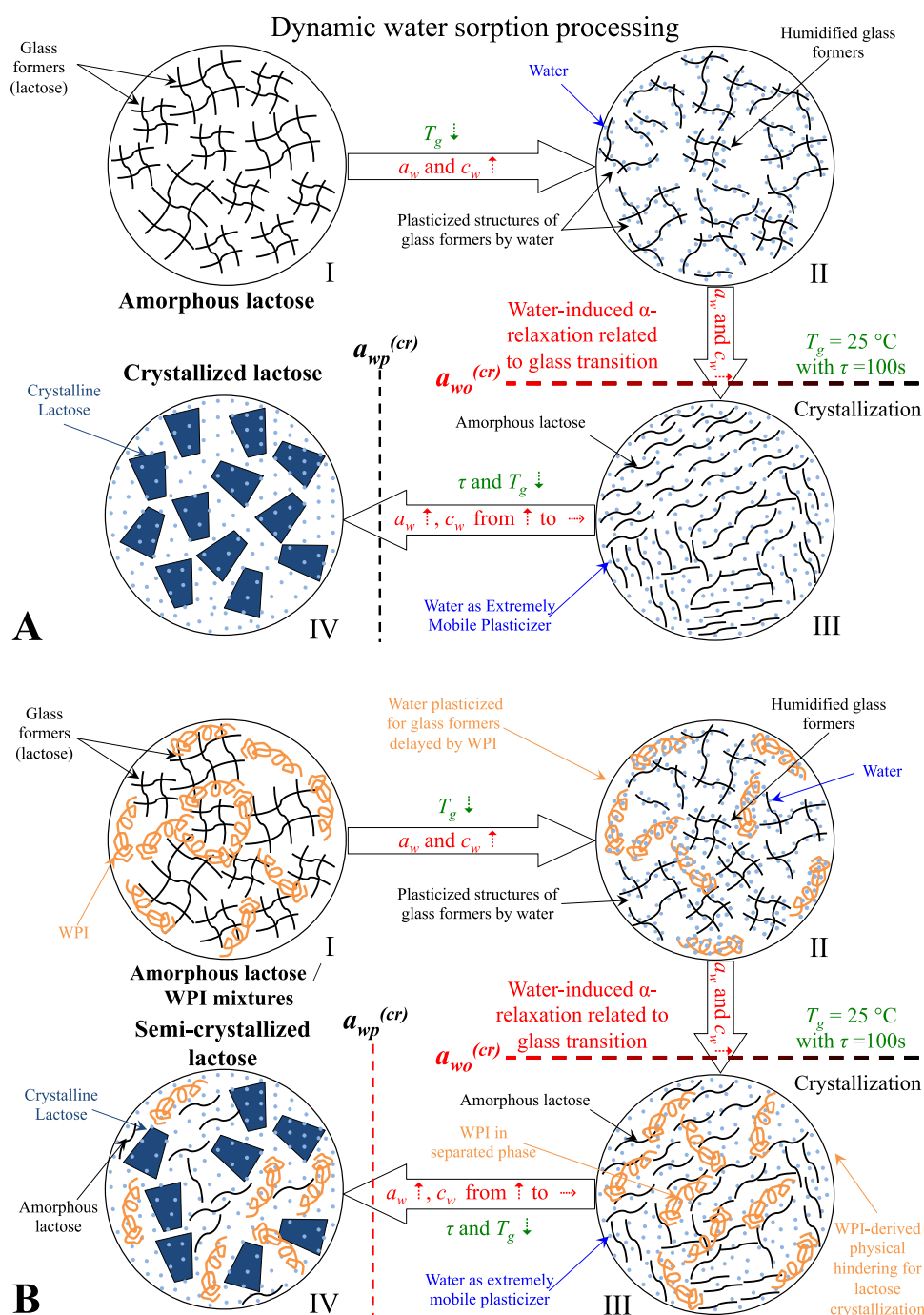
Figure 2. The comparison diagram between DDI and literature SSM data of freeze-dried lactose and lactose/WPI mixtures (7:3, 1:1 and 3:7, w/w) at flow rates of 300 ml/min at 25 °C (A-E). The $a_w^{(cr)}$ shows a highly linear relationship with lactose content ($R^2 > 0.98$) in lactose/WPI mixtures (F). The literature SSM sorption data were derived from Fan and Roos (2015).
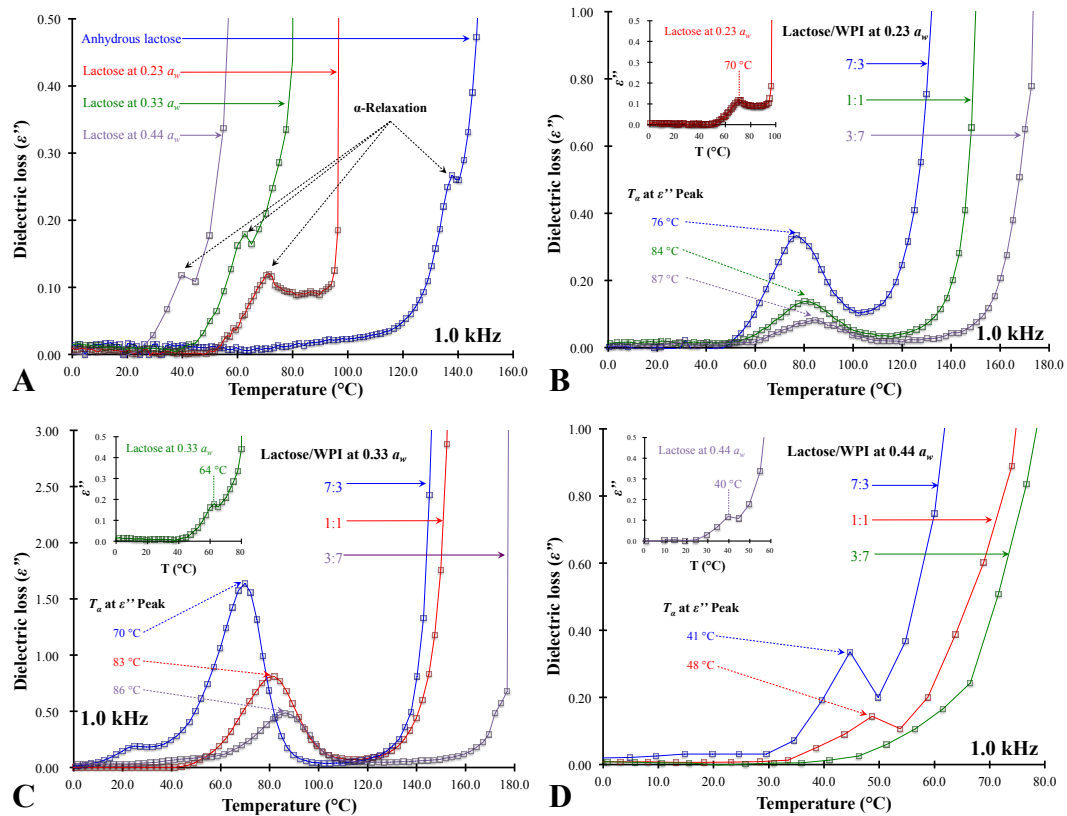
Figure 3. Schematic diagrams for water-induced α-relaxation and crystallization on amorphous lactose (A) and lactose/WPI mixtures (B) in dynamic water sorption processes, respectively. The symbols do not represent the real size and quantity of components.

Figure 4. The DEA spectra and peak temperature of ε'' as T_α of amorphous lactose (A) and lactose/WPI mixtures with 7:3, 1:1 and 3:7 mass ratios after storage at 0.23 a_w (B), 0.33 a_w (C), and 0.44 a_w (D) under 25 °C.
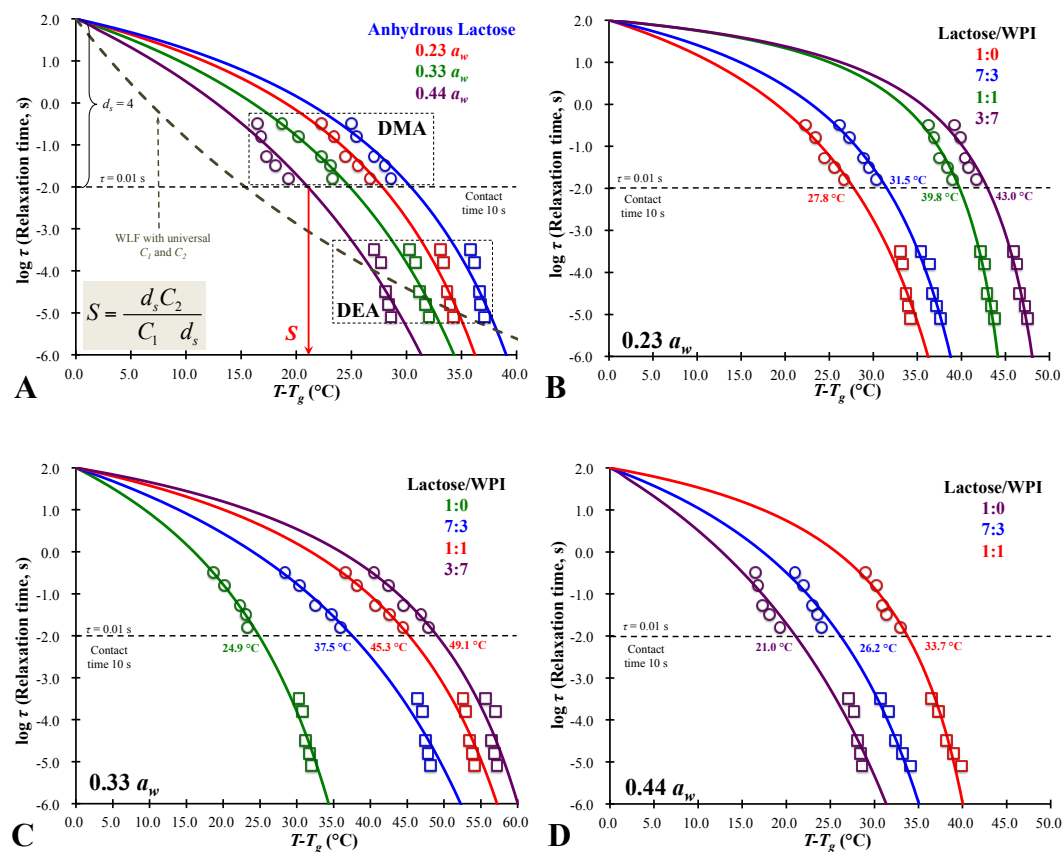
Figure

Figure 5. Strength parameters (S) of freeze-dried amorphous lactose at various water activities (0-0.44 a_w) (A), lactose/WPI mixtures at mass ratio of at 7:3, 1:1 and 3:7 at frequency of 1.0 kHz after storage at 0.23 a_w (B), 0.33 a_w (C) and 0.44 a_w (D) at $d_s = 4$ decreasing τ as measured using DEA and literature DMA (Fan & Roos, 2016c) down to 0.01 s. Such decrease in τ is known to result in particle stickiness and aggregation at a contact time of 10 s (Roos et al., 2015).
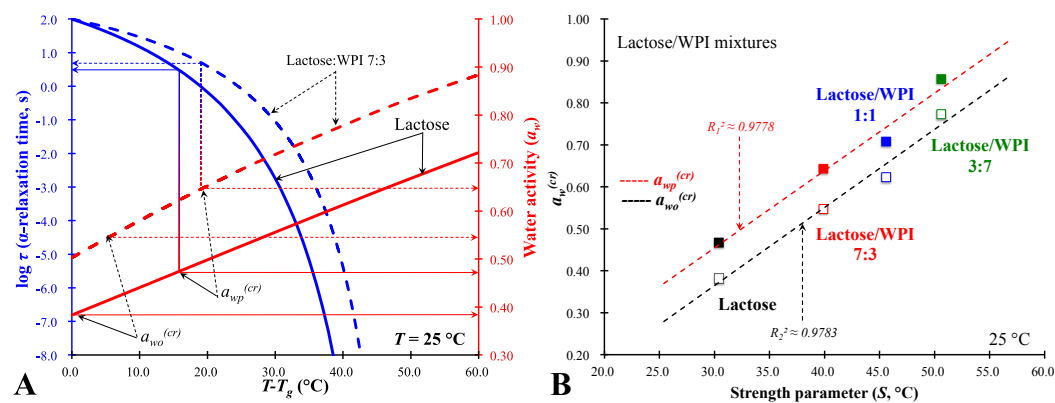
Figure 6. The relationship between a_w and $T\text{-}T_g$ of amorphous lactose and lactose/WPI mixture at 7:3 (w/w) with their corresponding relaxation times (A). B shows the relationship between strength parameter (S) and $a_w^{(cr)}$ for amorphous lactose and its WPI containing mixtures at 25 °C.

Figure Captions

Figure 1. The $a_w^{(cr)}$ for freeze-dried lactose respectively taking the peak a_w of first derivative $(a_{wp}^{(cr)})$ and onset a_w of the second derivative $(a_{wo}^{(cr)})$ on DDI sorption data at 25 °C (A). B shows the DDI curves for lactose and lactose/WPI mixtures with 7:3, 1:1 and 3:7 mass ratios by running at 25 °C, respectively.

Figure 2. The comparison diagram between DDI and literature SSM data of freeze-dried lactose and lactose/WPI mixtures (7:3, 1:1 and 3:7, w/w) at flow rates of 300 ml/min at 25 °C (A-E). The $a_w^{(cr)}$ shows a highly linear relationship with lactose content ($R^2 > 0.98$) in lactose/WPI mixtures (F). The literature SSM sorption data were derived from Fan and Roos (2015).

Figure 3. Schematic diagrams for water-induced α-relaxation and crystallization on amorphous lactose (A) and lactose/WPI mixtures (B) in dynamic water sorption processes, respectively. The symbols do not represent the real size and quantity of components.

Figure 4. The DEA spectra and peak temperature of ε'' as T_α of amorphous lactose (A) and lactose/WPI mixtures with 7:3, 1:1 and 3:7 mass ratios after storage at 0.23 a_w (B), 0.33 a_w (C), and 0.44 a_w (D) under 25 °C.

Figure 5. Strength parameters (S) of freeze-dried amorphous lactose at various water activities (0-0.44 a_w) (A), lactose/WPI mixtures at mass ratio of at 7:3, 1:1 and 3:7 at frequency of 1.0 kHz after storage at 0.23 a_w (B), 0.33 a_w (C) and 0.44 a_w (D) at $d_s = 4$ decreasing τ as measured using DEA and literature DMA (Fan & Roos, 2016c) down to 0.01 s. Such decrease in τ is known to result in particle stickiness and aggregation at a contact time of 10 s (Roos et al., 2015).

Figure 6. The relationship between a_w and T-T_g of amorphous lactose and lactose/WPI mixture at 7:3 (w/w) with their corresponding relaxation times (A). B shows the relationship between strength parameter (S) and $a_w^{(cr)}$ for amorphous lactose and its WPI containing mixtures at 25 °C.

Table 1. The onset and peak $a_w^{(cr)}$ for water-induced crystallization ($a_{wo}^{(cr)}$ and $a_{wp}^{(cr)}$) in freeze-dried lactose, lactose/WPI mixtures at 7:3, 1:1 and 3:7 mass ratios during DDI sorption process at 25 °C.

Table 2. The literature onset T_g, T_α at 1.0 kHz, material-specific C_1 and C_2, and S for freeze-dried lactose, lactose/ WPI mixtures at solid ratios of 7:3, 1:1 and 3:7 after storage at low a_w (≤ 0.44) at 25 °C.

Table

Table 1. The onset and peak $a_w^{(cr)}$ for water-induced crystallization ($a_{wo}^{(cr)}$ and $a_{wp}^{(cr)}$) in freeze-dried lactose, lactose/WPI mixtures at 7:3, 1:1 and 3:7 mass ratios during DDI sorption process at 25 °C.

Sample	Ratios	$a_{wo}^{(cr)}$	$a_{wp}^{(cr)}$
Lactose	-	0.381 ± 0.010^a	0.467 ± 0.003
Lactose/WPI	7:3	0.547 ± 0.018	0.643 ± 0.001
Lactose/WPI	1:1	0.623 ± 0.028	0.708 ± 0.006
Lactose/WPI	3:7	0.773 ± 0.013	0.857 ± 0.001

[a:] Values are mean ± SD (n=3)

Table 2. The literature onset T_g, T_α at 1.0 kHz, material-specific C_1 and C_2, and S for freeze-dried lactose, lactose/ WPI mixtures at solid ratios of 7:3, 1:1 and 3:7 after storage at low a_w (≤ 0.44) at 25 °C.

Sample	a_w	T_g	T_α	C_1	C_2	S
Lactose	0.00	105±3[a]	138±2	3.19±0.31	-54.63±0.63	30.4±0.7
	0.23	40±2	72±1[b]	3.47±0.23	-51.93±0.42	27.8±1.0
	0.33	30±3	64±3	4.93±0.19	-55.48±0.56	24.9±0.8
	0.44	14±1	40±1	7.66±0.45	-61.36±0.66	21.0±1.6
Lactose/WPI 7:3	0.23	40±1	76±1	2.38±0.33	-50.31±0.64	31.5±0.9
	0.33	30±1	70±1	5.15±0.21	-85.88±0.50	37.5±1.0
	0.44	13±1	41±3	4.13±0.35	-53.15±0.52	26.2±1.3
Lactose/WPI 1:1	0.23	41±1	84±1	0.98±0.43	-49.55±0.41	39.8±0.5
	0.33	30±2	83±1	2.87±0.44	-77.72±0.76	45.3±0.5
	0.44	14±2	48±5	1.83±0.25	-49.18±0.63	33.7±0.4
Lactose/WPI 3:7	0.23	41±2	87±0	1.07±0.38	-54.47±0.66	43.0±0.7
	0.33	30±3	86±4	2.30±0.29	-77.28±0.73	49.1±0.5
	0.44	13±2	N/A	-	-	-

[a]: The onset T_g of lactose and lactose/WPI mixtures are derived from Fan and Roos (2016c); [b]: Values are mean ± SD (n=3);

R-code and dataset(s) (.ZIP)

[Click here to download R-code and dataset(s) (.ZIP): R-code and datasets.zip](#)